DELINEATING THE DRIVERS OF GROUNDWATER FLOW AT A BACK BARRIER ISLAND – MARSH TRANSECT IN COASTAL GEORGIA

Jonathan Ledoux[1], Clark Alexander[2] and Christof Meile[1]

AUTHORS: [1]University of Georgia, Athens, Georgia; [2]Skidaway Institute of Oceanography, Savannah, Georgia
REFERENCE: *Proceedings of the 2013 Georgia Water Resources Conference*, held April 10–11, 2013, at the University of Georgia

Abstract. Groundwater plays an important role in coastal regions by delivering freshwater and nutrients to near shore and salt marsh environments. To quantify groundwater flow, salinity, temperature and pressure, sensors were installed in shallow piezometers along a transect behind Blackbeard Island, GA. Located approximately 90 m from the nearest tidal creek, the transect reaches from a back barrier island to a hammock and into the adjacent marsh. Coincident with each well, vibracores were taken and sediment permeability was estimated from grain size measurements. Combined with horizontal pressure gradients, this allowed quantification of groundwater flow. Subsequently, the impact of forces that govern groundwater movement such as tidal inundation, subsurface propagation of pressure signals, and variations in fluid density was assessed. First, the propagation of pressure in the subsurface was investigated using a one-dimensional model and was found to likely only have a minor effect at the location of the well transect. Then, measured pressure gradients were separated into contributions from piezometric head changes and density changes. Density changes were responsible for typically <10% of groundwater flow and the effect was most dominant at the hammock. To delineate the contribution of tidal flushing, a classical harmonic analysis of the pressure time series was performed. Results of this ongoing effort show that tidal flushing plays the primary role. Alternate drivers, including precipitation events, are most evident in periods with low tidal forcing. Understanding current drivers of groundwater movement will help predict hydrological response to changing forces and the potential for saltwater intrusion.

INTRODUCTION

Coastal salt marshes act as a buffer between terrestrial and marine ecosystems, connecting the coastal population and the ocean. Maintaining the stability of these environments is important as marshes provide habitat and remove dissolved chemical constituents. This process has long been recognized and employed in wastewater treatment of both surface flows (river, runoff) and groundwater.

It is important to consider the role of groundwater because it can influence the distribution of different vegetation (Ursino et al., 2004) and can be responsible for a potentially large fraction of nutrient fluxes to the coastal ocean (Swarzenski et al., 2007). Quantifying the different drivers of groundwater flow can help predict future changes in groundwater dynamics due to urbanization or climate change. Together these two factors have the ability to completely change the southeast coasts within the next century.

The groundwater beneath Blackbeard Island and Sapelo Island is fresh, with salinities near 0 ppt, while the water regularly inundating the marsh is near 35 ppt. These two distinct water bodies mix beneath the marsh or hammock and form waters that can range from brackish to hypersaline (60 ppt) because of evapotranspiration. Certain vegetation species are able to tolerate these high salinity environments (Mendelssohn and Morris 2000). Despite the ability of a salt marsh to exist with such wide salinity gradients, this environment is still threatened. Craft et al. (2009) predicted that sea level rise (SLR) could cause up to 45% of salt marshes to decline from present day amounts due to inundation. SLR will not only drown a marsh, but it may also alter groundwater flow patterns.

In a salt marsh-hammock environment, there are several drivers of groundwater flow. On the rising tide, a pressure wave is propagated through the subsurface of the marsh, influencing groundwater flow. Differences in fluid temperature and salinity give rise to density-driven flow, with groundwater discharge where the freshwater-saltwater interface dips below the freshwater lens beneath hammocks and barrier islands. In addition, high temperatures can cause a high amount of evaporation across the marsh, and salinities in saltpans can reach 60 ppt during parts of the year, potentially inducing salt fingering. Finally, wind and low-pressure systems can alter the ocean water level, thereby affecting pressure gradients in both shallow and deep aquifers.

In this communication we show a time series of pressure data from a well transect from Blackbeard Island, a barrier island at the Georgia coast, across a marsh section containing saltpans, to a hammock and into a salt marsh adjacent to a tidal creek. We present an analysis of some of the above-mentioned driving forces for groundwater

flow and assess their relative importance and briefly discuss implications under changing climatic conditions.

METHODS

Study site and data

The study site is located on a small hammock located on the west side of Black Beard Island on the Georgia coast. This hammock was formed in the Holocene era according to luminescence and C14 dating from vibracores taken at the site (Turck and Alexander 2013). Across the hammock, between Blackbeard Island and the creek, a transect of 9 wells has been installed as part of the Georgia Coastal Ecosystems – Long Term Ecological Research (GCE-LTER). These wells vary from a depth of 1.50 m to 3.52 m to the ground surface and extend over a distance of about 130 m (Figure 1). Each well was equipped with a data logger, recording temperature, salinity, and pressure every fifteen minutes from August 2011 to June 2012. Each logger was installed 0.25 m from the bottom of each well. Every well has a screened height of 0.30 m from the bottom of the well. Adjacent to every well, a vibracore was collected. Measurements such as grain size and % sand, silt, and clay were taken, and the core stratigraphy gives an exact location of the depth of the low-permeability mud layer at each well. At well locations 1, 3, 5 and 8, slug tests were performed to acquire hydraulic conductivity and permeability.

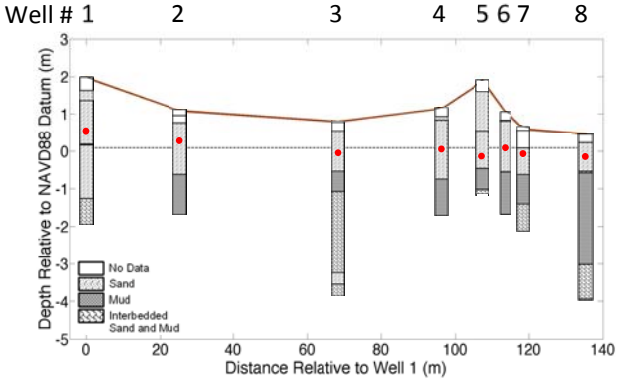

Figure 1: Cross sectional view of well locations and sensor depths (red dots) relative to NAVD88. The average sensor depth (0.09 m) is indicated by the horizontal dashed line. Vibracore results are shown with stratigraphy units. Surface topography is indicated by the brown line.

Subsurface pressure wave propagation

One of the drivers of groundwater flow is the propagation of a pressure wave through the marsh subsurface. The extent and speed at which this occurs can be expressed as (Schultz & Ruppel 2002):

$$h(x,t) = b + \sum_{j=1}^{\omega_N} A_j \exp\left[-x\sqrt{\frac{\omega_j}{2D}}\right]\cos\left(\omega_j t - \Phi_j - x\sqrt{\frac{\omega_j}{2D}}\right) \quad (1)$$

where A, ω, and Φ describe the tidal signal typical for the study site, D is diffusivity set to 0.0048 $m^2\ s^{-1}$, calculated as D=K*b/S where b is the average saturated thickness set to 1.5 m, K the hydraulic conductivity of 2.3 $*10^{-5}$ m/s, determined by slug test at well 8 and S is storativity, set to 0.2 (Schultz & Ruppel 2002).

Data treatment

Due to the variability in the vertical location of each sensor, the acquired data was first referenced to a common depth. In order to reduce the amount of error associated to each correction, due to possible vertical salinity changes, the average well depth was chosen. Measured pressure was referenced to that depth using densities computed by the UNESCO algorithms (UNESCO 1983) based on the measured salinity and temperature in the well.

Darcy's Law and the decomposition of pressure signals

Groundwater flow depends on properties of the porous media, the fluid and the pressure gradient. In one dimension, flow along the x-axis can be expressed as (Bear 1972):

$$q = -\frac{k}{\mu} * \frac{\partial P}{\partial x} \quad (2)$$

where q is the Darcy flow velocity (m/s), k is intrinsic permeability (m^2), μ is the dynamic viscosity (Ns/m^2), and $\frac{\partial P}{\partial x}$ is the pressure gradient (N/m^3) with respect to x. The measured pressure (P^m) can be broken into two different components, separating the effect of density variations on pressure (P^d) from piezometric head (P^h)

$$P^m = P^h + P^d \quad (3)$$

Pressure can be expressed as

$$P = \rho g h \quad (4)$$

where ρ is density (kg/m^3), h denotes the head (m) and g is gravitational acceleration (m/s^2). One can decompose both the head and the density into a reference head and density (h_{avg}, ρ_{avg}) and a deviation from it (h', ρ'), respectively, so that

$$P = (\rho_{avg} + \rho')g(h_{avg} + h') \quad (5)$$

The pressure gradient can then be written as:

$$\frac{\Delta P^m}{\Delta x} = \frac{((\rho_{avg}+\rho_2')g(h_{avg}+h_2'))}{x_2 - x_1} - \frac{((\rho_{avg}+\rho_1')g(h_{avg}+h_1'))}{x_2 - x_1} \quad (6)$$

where the subscripts 1 and 2 denote two adjacent wells. Multiplying through and cancelling will result in:

$$\frac{\Delta P^m}{\Delta x} = \frac{(\rho_{avg} g(h_2' - h_1'))}{x_2 - x_1} + \frac{(h_{avg} g(\rho_2' - \rho_1'))}{x_2 - x_1} + \frac{(g(\rho_2' h_2' - \rho_1' h_1'))}{x_2 - x_1} \quad (7)$$

Choosing the reference density and head to be the average between the two wells,

$$h_2' = -h_1' = \frac{\Delta h}{2} \quad (8)$$

$$\rho_2' = -\rho_1' = \frac{\Delta \rho}{2} \quad (9)$$

results in

$$\frac{\Delta P^m}{\Delta x} = \frac{(\rho_{avg} g \Delta h)}{x_2 - x_1} + \frac{(h_{avg} g \Delta \rho)}{x_2 - x_1} \quad (10)$$

Hence, the piezometric pressure gradient is:

$$\frac{\Delta P^h}{\Delta x} = \frac{(\rho_{avg} g \Delta h)}{x_2 - x_1} \quad (11)$$

and the density-driven flow component is associated with

$$\frac{\Delta P^s}{\Delta x} = \frac{(h_{avg} g \Delta \rho)}{x_2 - x_1} \quad (12)$$

Harmonic analysis using T_tide

To achieve a better understanding of how tidal inundation is influencing the system at each well, the Matlab package T_tide (Pawlowicz et al., 2002) was used. It utilizes 45 astronomical and the 24 most important shallow water constituents to create the tidal signal. When a signal processed with this script, T_tide is able to identify the amplitude and phase shift that correspond to each of the tidal constituents. This analysis can be conducted upon the pressure gradient between adjacent wells, because the time series of the difference between two tidally driven pressure signals with a slight temporal offset exhibits the same frequencies as the tidal signal in the pressure record itself.

RESULTS

Subsurface pressure wave propagation

Figure 2 shows the impact of the propagation of the tidal signal through the subsurface using equation 1. When there is a tidal amplitude of 0.75 m, the influence of propagation extends roughly 20 m from the nearest tidal creek into the marsh.

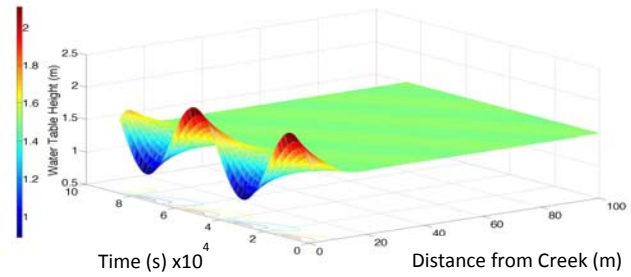

Figure 2: Propagation of the tidal signal through the subsurface.

Decomposition of density and piezometric head

There are two main factors that directly affect the pressure gradient: changes in fluid density and changes in piezometric head. Separation of the two highlights which component controls groundwater flow in different sections of the salt marsh.

Equations 11 and 12 result in two separate pressure gradients between each well pairings, one due to density variations (eq. 12), the other due to head changes (eq. 11). In figure 3, the pressure gradient due to density changes show that gradients between wells can be pointing in opposite directions.

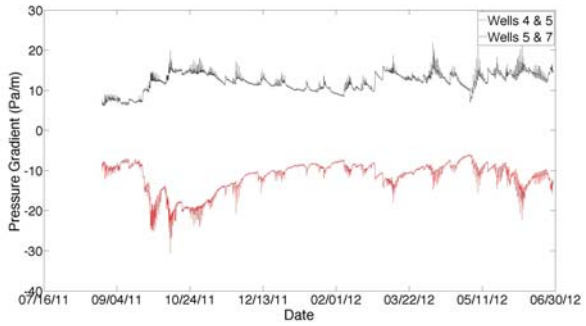

Figure 3: Pressure gradients due to density changes between wells 4 & 5 (red) and wells 5 & 7 (black).

Identification of tidal inundation

The pressure gradients with density changes removed were processed using the T_tide (Figure 4A&B). Fitting the known frequencies, the amplitude and phase shift for the tidal signal was calculated and output as an artificial tidal signal (Figure 4C&D). This method was applied to all the well gradients, however only examples from wells 1-2 and wells 7-8 are shown.

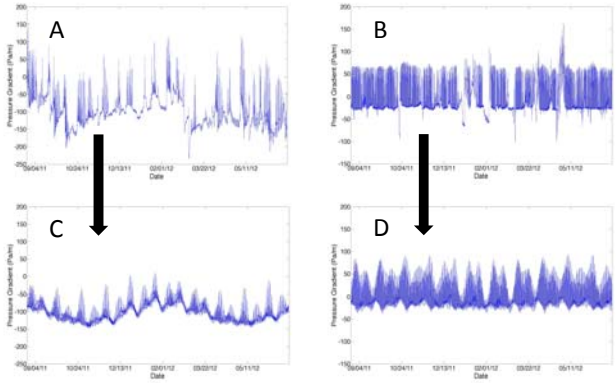

Figure 4: Pressure gradients due to piezometric head changes between wells 1 and 2 (A) and wells 7 and 8 (B). Estimated tidal signal from pressure signal due to piezometric head changes between wells 1 and 2 (C) and wells 7 and 8 (D).

DISCUSSION

The piezometer closest to the tidal creek (Well 8) is located well beyond the 20 m distance of influence (Figure 2) of pressure propagation through the subsurface, indicat-

ing that the subsurface pressure wave associated with the changing creek water level will have little impact on groundwater flow. Tidal inundation of the marsh platform, however, will also push a pressure wave through the subsurface, though its magnitude is likely negligible compared to the direct effect of tidal loading.

Density's role in driving groundwater flow may also not be a large factor in a salt marsh with low hydraulic conductivity (Martin 1996). The pressure gradient due to density changes is an order of magnitude smaller (Figure 3) than the pressure gradient due to piezometric head changes (Figure 4). The well transect consists of three salinity zones; Blackbeard Island (freshwater), hammock (brackish) and marsh (salty), with potential for density driven flow at their intersections. Density-driven flow has up to a 16% influence between wells 4 and 5, located at the marsh-hammock interface. This substantial contribution is largely due to the strong salinity gradient, along with similar piezometric heads in the two wells.

With density effects quantified and removed from the pressure gradient, the remaining drivers can be separated and quantified. In a system that regularly gets inundated, it is likely that tidal inundation plays a large role in groundwater flow. There is a large difference in the tidal signal across our transect (Figure 4A&B). Wells 7 and 8, closest to the tidal creek, are regularly inundated. Wells 1 and 2, closest to Blackbeard Island, only get inundated on the largest tides and have a freshwater head influence.

The difference in the magnitudes between Figure 4A&B can be explained by their location and surface topography (Figure 1). For wells 7 and 8, the generated tidal signal has a similar magnitude as the pressure gradient. This suggests that tidal inundation is the most important driver at this location. In contrast, for wells 1 and 2, located the farthest away from the tidal creek, this is not the case. The tidal signal's magnitude is much lower than the derived signal. This could mean that a freshwater head existing from Blackbeard Island is having a large impact at this location.

The influence of precipitation can be seen in the pressure data from wells 1 and 2, located closest to Blackbeard Island. Figure 5 compares the individual well responses, the pressure gradient, and the precipitation data during that time frame. Well 1 has a larger response to the two precipitation events than well 2. This is due to well 1 being less frequently inundated as well as receiving a large influence of the freshwater head from Blackbeard Island. This larger response in well 1 shifts the pressure gradient by almost 150 Pa/m for each event.

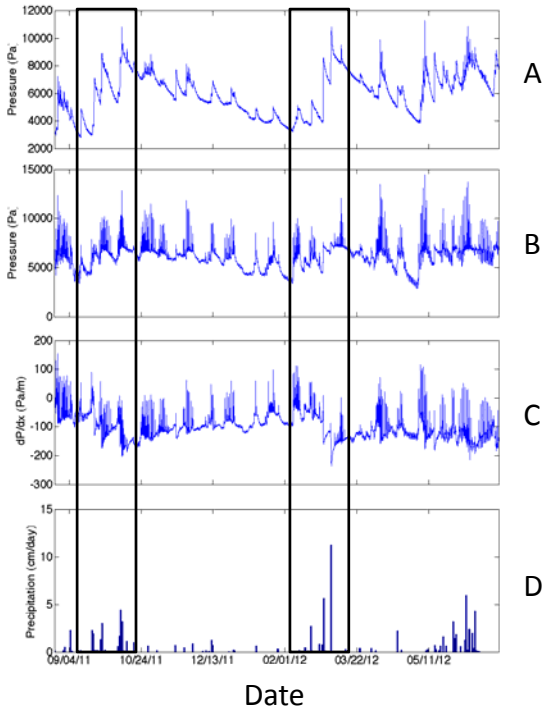

Figure 5: Measured pressure response for well 1 (A) and well 2 (B). Pressure gradient due to piezometric head changes between wells 1 and 2 (C). Daily precipitation totals (D).

CONCLUSION

Groundwater flow plays an important role for the coastal ecosystem. Understanding what controls groundwater flow will help make predictions of how water resources may change during global climate change and SLR. Using temperature, salinity, and pressure data, it is possible to quantify and compare different drivers in a marsh setting. The effect of density variations on groundwater flow can be constrained using mathematical manipulations. The role of density on groundwater flow can have up to a 16% influence. For the wells located on the lower marsh, tide has the largest contribution to the total flow. Groundwater flow towards Blackbeard Island appears to have additional factors controlling groundwater flow. Quantifying the remaining drivers is the next step in better understanding this dynamic system.

In Georgia, the coast consists of a series of barrier islands, salt marshes, and tidal creeks. Since the southeast has the fastest growing population of all the coastal regions (Crossett et al., 2004), this habitat may be threatened by urbanization, due to the associated impact on surface runoff, groundwater infiltration and changes in nutrient loadings. This, together with SLR has the potential of affecting coastal marshes, and future work is aimed at quan-

tifying such effects on groundwater flow dynamics in the transition between barrier island and adjacent marshes.

ACKNOWLEDGMENTS

We would like to thank Wade Sheldon for maintaining the LTER database and Caroline Reddy and Jacob Shalack for data collection. This study was supported by the NSF funded Georgia Coastal Ecosystems Long Term Ecological Research program (GCE-LTER, OCE-1237140).

REFERENCES

Craft C., Clough J., Ehman J., Joye S., Park R., Pennings S., Guo H., Machmuller M. (2009) Forecasting the effects of accelerated sea-level rise on tidal marsh ecosystem services. *Frontiers in Ecology and the Environment*, **7(2)**, 73-78.

Baustian J., Mendelssohn I., Hester J. (2012) Vegetation's importance in regulating surface elevation in a coastal salt marsh facing elevated rates of sea level rise. *Global Change Biology*, **18**, 3377-3382.

Crossett D., Culliton T., Wiley P., Goodspeed T. (2004) Population rends along the coastal United States: 1980-2008. *National Oceanic and Atmospheric Administration Coastal Trends Report Series*, 54.

Pawlowicz R., Beardsley B., Lentz S. (2002) Classical tidal harmonic analysis including error estimates in MATLAB using T_TIDE. *Computers & Geosciences*. **28**, 929-937.

Martin J. (1996) Hydrology and pore-water chemistry of a tidal marsh, Fraser River estuary. MSc thesis, Simon Fraser University, 132 pp.

Schultz G., Ruppel C. (2002) Constraints on hydraulic parameters and implications for groundwater flux across the upland-estuary interface. *Journal of Hydrology*, **260**, 255-269.

Swarzenski P., Simonds F., Paulson A., Kruse S., Reich C. (2007) Geochemical and geophysical examination of submarine groundwater discharge and associated nutrient loading estimates into Lynch Cove, Hood Canal, WA. *Environmental Science Technology*, **41**, 7022-7029.

UNESCO (1983). Algorithms for computation of fundamental properties of seawater. UNESCO technical papers in marine science 44.

Ursino N., Silvestri S., Marani M. (2004) Subsurface flow and vegetation patterns in tidal environments. *Water Resources Research*, **40**, W05115, doi: 10.1029/2003WR002702.

Turck, J. and Alexander, C. (2013). Coastal Landscapes and Their Relationship to Human Settlement on the Georgia Coast. Anthropological Papers of the American Museum of Natural History. In press.